Challenges in Sustainability
https://www.acadlore.com/journals/CIS

Urban Expansion and Its Dual Impact on Biodiversity Loss and Thermal Dynamics: A Remote Sensing-Based Assessment of Abomey-Calavi, Benin

Cossi Jeannot Melchior Kadja[1,2*], Iléri Dandonougbo[2], Ayira Korem[3], Marcel Adigbegnon[4], François Teadoum Naringué[1,2], Benjamin Sotondji Allagbe[5]

[1] Regional Centre of Excellence on Sustainable Cities in Africa (CERVIDA-DOUNEDON), University of Lomé, 01 BP 1515 Lomé, Togo
[2] Research Laboratory on Spaces Exchanges and Human Security (LaREESH), University of Lomé, 01 BP 1515 Lomé, Togo
[3] Faculty of Economics and Management, University of Lomé, 01 BP 1515 Lomé, Togo
[4] Laboratory of Climatology and Tropical Ethnoclimatology, University of Abomey-Calavi, 01 BP 526 Abomey-Calavi, Benin Republic
[5] Urban and Rural Dynamics Laboratory (LEDUR), University of Abomey-Calavi, 01 BP 787 Abomey-Calavi, Benin Republic

[*] Correspondence: Cossi Jeannot Melchior Kadja (cossi.kadjar@cervida-togo.org)

Received: 04-03-2025 **Revised:** 05-28-2025 **Accepted:** 07-18-2025

Citation: Kadja, C. J. M., Dandonougbo, I., Korem, A., Adigbegnon, M., Teadoum Naringué, F., & Allagbe, B. S. (2025). Urban expansion and its dual impact on biodiversity loss and thermal dynamics: A remote sensing-based assessment of Abomey-Calavi, Benin. *Chall. Sustain.*, *13*(3), 412–424. https://doi.org/10.56578/cis130307.

Abstract: Rapid urban expansion in sub-Saharan Africa has increasingly posed challenges to ecological sustainability and climatic stability. In this study, the spatiotemporal impacts of urban growth on biodiversity and surface temperature dynamics in Abomey-Calavi, Republic of Benin, were quantitatively assessed. A multi-decadal analysis was conducted using satellite imagery from the Landsat series (1992, 2002, 2012, and 2022), temperature records, and relevant literature, in alignment with Sustainable Development Goal (SDG) Indicator 11.3.1 and Indicator 1 of the Singapore City Biodiversity Index (CBI). Findings revealed a significant imbalance between land consumption and population growth, with a land use to population ratio of 4.25, substantially exceeding the sustainable threshold of 1. This trend denotes unsustainable urban development. Concurrently, biologically active land—serving as a proxy for biodiversity—declined from 472.42 km² (94.75% of the study area) in 1992 to 220.31 km² (44.19%) in 2022, amounting to a biodiversity area loss exceeding 50%. Thermal analysis detected statistically significant shifts in both minimum and maximum temperatures, with minimum temperatures increasing from 24.41℃ to 25.14℃ ($p = 3.14 \times 10^{-5}$) and maximum temperatures rising from 30.30℃ to 31.02℃ ($p = 7.62 \times 10^{-5}$). These findings indicate that urban sprawl has not only driven ecological degradation through habitat fragmentation and biodiversity depletion but has also exacerbated the urban heat island effect. The methodological integration of geospatial analysis, climate data, and urban biodiversity indicators demonstrates the utility of multidisciplinary approaches in diagnosing the environmental consequences of unregulated urbanization. The results underscore an urgent need for evidence-based urban planning and biodiversity-sensitive development policies tailored to rapidly expanding West African cities.

Keywords: Urban biodiversity loss; Land use efficiency; Remote sensing; Sustainable Development Goal (SDG) Indicator 11.3.1; Singapore City Biodiversity Index (CBI); Abomey-Calavi; West Africa; Urban sprawl

1. Introduction

Uncontrolled urban sprawl and its direct and indirect consequences are urgent challenges to sustainability (Emadodin et al., 2016) and for countries and governments. In recent years, this has become a topic of interest worldwide (Terfa et al., 2019). Many studies have been conducted on urban sprawl in metropolitan cities worldwide (Olanrewaju & Adegun, 2021; Yiran et al., 2020). Various studies on urban sprawl highlight several

weaknesses in the realities they highlight. Indeed, almost every aspect of life is affected by the challenges raised by this phenomenon, including social, legal, and economic concerns; infrastructure (particularly those linked to transport); and the environment (Cao et al., 2024). Land use resulting from urban sprawl influences environmental degradation (Putra et al., 2021). The local climate is heavily affected by rapid, uncontrolled urban sprawl, and substantial changes have been observed as urbanization has led to various climatic disturbances in recent decades. Urbanization has continued to accelerate from the Industrial Revolution to the present day. This trend has evolved over the coming years and decades (United Nations Department of Economic & Social Affairs, 2019). Thus, SDG 11 aims to achieve "sustainable cities and communities", and is designed to make cities safe, resilient, and inclusive (UN-Habitat, 2021).

African cities, like those on other continents, are affected by this trend and are subject to urban growth, whose speed varies according to local particularities. Indeed, by 2050, African cities will be home to approximately 900 million people (United Nations Department of Economic & Social Affairs, 2019), with increased housing and infrastructure needs (Olanrewaju & Adegun, 2021; Yiran et al., 2020). The work of Yiran et al. (2020) on urban sprawl in sub-Saharan Africa showed that the consequences of urban growth are diverse, with specific features depending on the country and city studied. For example, in Ghana, environmental consequences include the destruction of vegetation and open spaces, and the development of unsustainable housing (Cobbinah & Aboagye, 2017). Several studies have been conducted on the impact of urban growth on the environment in Africa (Olanrewaju & Adegun, 2021; Thomas & Whittington, 2023). The relationship between urban growth and the environment has been highlighted (Li et al., 2022). The literature shows a positive correlation between urban growth and environmental changes in Africa (Teadoum Naringué et al., 2025; Thomas & Whittington, 2023). Nevertheless, there are limited studies on the influence of urban growth on the tripartite relationship between urban growth, biodiversity, and temperature in West African secondary cities.

Abomey-Calavi, a district in the south of the Republic of Benin, is experiencing constant urban growth owing to the urbanization of its eastern neighbor, Cotonou (Osseni et al., 2023). Indeed, its intercensal growth rate was estimated at 6.93% between 2002 and 2013 (INSAE, 2016), making it one of the most densely populated cities in Benin, accounting for 46.9% of the population of the Atlantic Department. This growing population has led to rapid urban growth with noticeable consequences for both biodiversity and temperature. Abomey-Calavi studied the consequences of urban growth on the environment as well as the importance of vegetation in urban environments (Osseni et al., 2023). Lopez et al. (2017) showed a correlation between temperature and biodiversity in Abomey-Calavi.

Very few studies have addressed the simultaneous impact of urban growth on biodiversity and temperature in the Benin Republic. It is important to fill this gap in scientific research to guide decision makers, researchers, and urban planners in proposing urban policies that can reduce the impacts of urban growth on biodiversity and temperature. The present study aims to contribute to reducing this gap by assessing the impacts of urban growth on urban biodiversity and temperature in Abomey-Calavi, Republic of Benin. First, it assesses the effectiveness of urban growth. Second, it analyzes the evolution of urban biodiversity and temperature. Finally, it analyzes the correlations between these different phenomena.

2. Methodology

2.1 Study Area

The district of Abomey-Calavi is located in the south of the Republic of Benin in West Africa, and covers an area of 593 km². According to data from the Institut National de la Statistique et de la Démographie (INStaD), the district's population was 656,358 in 2013, with an intercensal growth rate of 6.93% (INSAE, 2016). It is located between 6°22' and 6°30' North latitude and between 2°15' and 2°22' East longitude and has a relatively flat relief with a ground composed of sandy plains and bare plateaus interspersed with depressions and swamps. The territory is bordered to the north by the district of Zè, to the south by the Atlantic Ocean, and to the west by the districts of Ouidah and Tori-Bossito. To its east lie Lake Nokoué, the district of So-Ava, and Cotonou (the economic capital of the Republic of Benin), as shown in Figure 1.

2.2 Materials

To assess urban growth, aerial images from the Landsat 5 Thematic Mapper (TM), Landsat 7 Enhanced Thematic Mapper Plus (ETM+), and Landsat 8 Operational Land Imager (OLI) satellites were used for the respective years. The analysis years defined for this study were 1992, 2002, 2012, and 2022, to enable a comparative analysis over time. All images used had a resolution of 30m × 30m, with less than 10% cloud cover. The images were acquired from the United States Geological Survey (USGS) and are freely available at https://earthexplorer.usgs.gov/.

Several scientific studies on urban growth have been conducted using Landsat satellite data (Teadoum Naringué

et al., 2025; Waseem et al., 2021). We chose Landsat satellites because they are freely available, have good spatial resolution, and cover a wide period, including our study period.

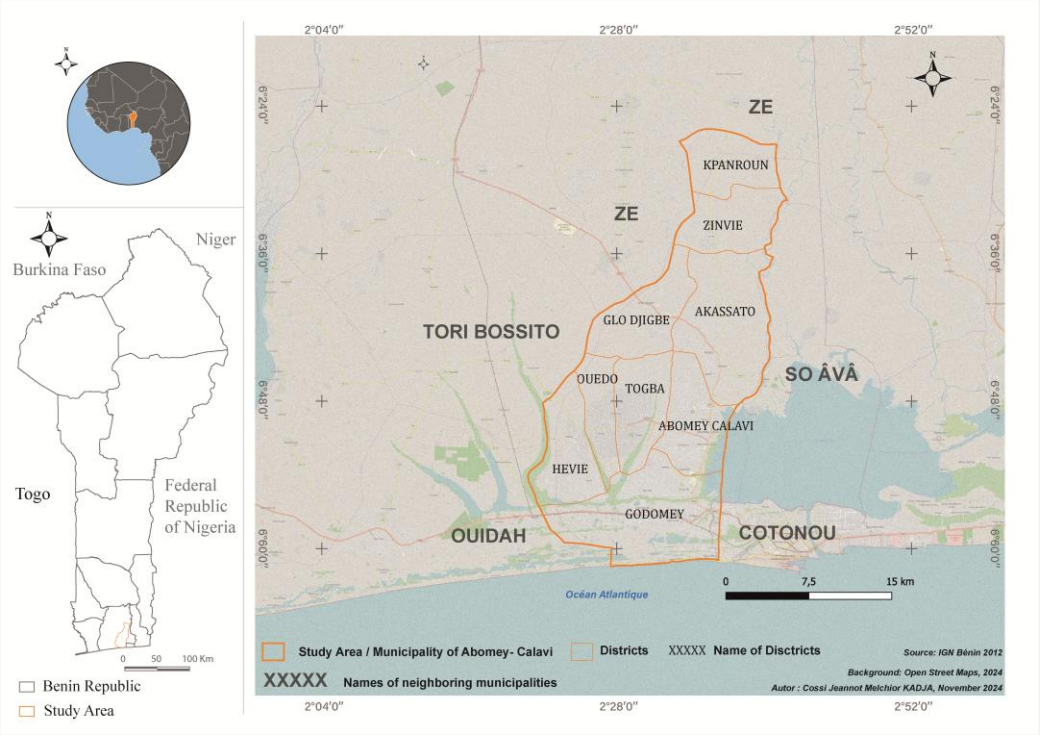

Figure 1. Study area map

2.3 Methods

Four (04) types of spaces were defined to assess changes in land use. These were water, vegetation, agricultural land, bare land, and built-up areas, whose indices were evaluated. A similar method was used by Waseem et al. (2021). Table 1 lists the composition of each space presented in this study.

Table 1. Spaces and compositions

Spaces	Compositions
Water	All aquatic elements: lakes, lagoons, oceans
Vegetation	Open forest, dense forest, open forest, tree and shrub savannahs, crops and fallow land with trees, plantations
Built up area	Buildings, agglomerations
Bare lland	Bare floors

2.3.1 Satellite imagery processing

The first step in image processing is to calculate indices. These were the Normalized Difference Water Index (NDWI), Normalized Difference Vegetation Index (NDVI), and Normalized Difference Built-up Area Index (NDBI).

Aerial imagery from different periods is also used. These are 1992, 2002, 2012, and 2022. In these images, urban development was distinguished from other categories. The green and near-infrared channels are used to create NDWI to identify water surfaces and map the water itself. The water range was obtained using Eq. (1) and Eq. (2) (Waseem et al., 2021).

$$\mathrm{NDWI} = \frac{(\mathrm{Green} - \mathrm{NIR})}{(\mathrm{Green} + \mathrm{NIR})} \quad (1)$$

$$\mathrm{LWM} = \mathrm{IR\ Green} \times 100 \quad (2)$$

where, NIR stands for Near Infrared and IR for Infrared, Green represents the ground reflectance of the green

channel.

The NDVI value generally varies between -1 and +1. The reflection of vegetation was greater than that in the visible bands (Konkobo & Somé, 2023). Here, the vegetation index was extracted by deducting the near-infrared (NIR) red band and then dividing the sum of the NIR and red bands in all Landsat images. The formula for calculating the NDVI is given in Eq. (3).

$$\mathrm{NDVI} = \frac{(\mathrm{NIR} - \mathrm{Red})}{(\mathrm{NIR} + \mathrm{Red})} \tag{3}$$

The built-up area index is defined based on Eq. (4) below. The built-up area index is defined by subtracting the short-wave infrared spectral band from the near-infrared band.

$$\mathrm{NDBI} = \frac{(\mathrm{SWIR} - \mathrm{NIR})}{(\mathrm{SWIR} + \mathrm{NIR})} \tag{4}$$

Short-Wave Infrared (SWIR) is a type of short-wave infrared spectral band.

The following formula was used to calculate the built-up area: This formula subtracts the built-up area index by normalizing the difference from the vegetation index using the NDVI. The built-up area was obtained using Eq. (5).

$$\mathrm{BUA} = \mathrm{NDBI} - \mathrm{NDVI} \tag{5}$$

Table 2 summarizes the spectral bands used, by satellite and by year.

Table 2. Spectral band used by satellite and by year

Years	Landsat Sensor	NDVI (Red and NIR)	NDWI
1992	Landsat 5	Band 3 (Red): 0.63-0.69 µm Band 4 (NIR): 0.76-0.90 µm	Band 4 (NIR): 0.76-0.90 µm Band 5 (SWIR): 1.55-1.75 µm
2002	Landsat 7 ETM+	Band 3 (Red): 0.63-0.69 µm Band 4 (NIR): 0.77-0.90 µm	Band 4 (NIR): 0.77-0.90 µm Band 5 (SWIR): 1.55-1.75 µm
2012	Landsat 7 ETM+	Band 3 (Red): 0.63-0.69 µm Band 4 (NIR): 0.77-0.90 µm	Band 4 (NIR): 0.77-0.90 µm Band 5 (SWIR): 1.55-1.75 µm
2022	Landsat 8 (OLI)	Band 4 (Red): 0.64-0.67 µm Band 5 (NIR): 0.85-0.88 µm	Band 5 (NIR): 0.85-0.88 µm Band 6 (SWIR): 1.57-1.65 µm

Table 3. Selection of ROI for each class

Class	NDBI	NDWI	NDVI	Bare Land	Total Line
Selected ROI_1992					
NDBI	32	2	0	6	40
NDWI	0	40	0	0	40
NDVI	0	1	39	0	40
Bare Land	5	0	0	35	40
Total Column	37	43	39	41	160
Selected ROI_2002					
NDBI	39	0	0	1	40
NDWI	1	38	0	1	40
NDVI	0	6	29	5	40
Bare Land	5	0	0	35	40
Total Column	45	44	29	42	160
Selected ROI_2012					
NDBI	39	0	1	0	40
NDWI	0	39	0	1	40
NDVI	0	5	35	0	40
Bare Land			3	37	40
Total Column	39	44	39	38	160
Selected ROI_2022					
NDBI	36	0	4	0	40
NDWI	0	38	2	0	40
NDVI	0	1	39	0	40
Bare Land	0	0	5	35	40
Total Column	36	39	50	35	160

The second processing step involves image classification. The various indices were combined for a preliminary visualization of the natural color (true color) by associating the red (B4), green (B3), and blue (B2) bands.

Following this step, training plots Region of Interest (ROI) were created on the raster image resulting from the combination of indices using the ROI tool of the Semi-automatic Classification Plugin (SCP) of QGIS 3.34.12. ROIs between 140 and 180 were defined for each study year. Details of the sample size for each class are given in Table 3. The training areas were selected based on field observations and Google Earth Pro orthophotos. The information gathered is used to train the classification algorithm. Once the samples were prepared, a classification algorithm was developed. The Maximum Likelihood Classifier (MLC) algorithm was selected, and the macro-class option was activated in the SCP interface. The MLC algorithm was chosen for its high performance, robust results, and low risk of classification errors (Saikrishna & Sivakumar, 2022). The algorithm was used in QGIS 3.34.12.

2.3.2 Assessment of overall accuracy and Kappa coefficient

The overall accuracy is important for ensuring the quality of the classification results. This was assessed by reference points and field checks, using GPS tools and ArcGis 10.8 software. The Kappa coefficient, used to validate the results, is a discrete multivariate technique that is used to assess the accuracy of the results. Kappa coefficients above 0.80 are considered excellent accuracies (Teadoum Naringué et al., 2025). The formula for calculating this is shown in Eq. (6) (Wei et al., 2024).

$$k=\frac{P_{\text{accord}}-P_{\text{hasard}}}{1-P_{\text{hasard}}} \tag{6}$$

where:

P_{accord}=Percentage of the number of measurements consistent between raters;

P_{hasard}=Percentage of the number of measurement changes between raters.

2.3.3 Land consumption per capita (LCPC) and land consumption rate relative to the population growth rate (LCRPGR)

For the various calculations, we used the UN Data Directory on Sustainable Development (United Nations, 2025), available online at https://unstats.un.org/sdgs/metadata. In this study, we mainly used the template for the indicator linked to target SDGs 11.3.1 (Combary et al., 2024).

Land consumption per capita (LCPC) indicates the surface area used by each inhabitant in the study area at a given time. Thus, they can be used to understand changes within the same city (Combary et al., 2024).

$$\text{LCPC}=\frac{\text{BUA}_t}{\text{Pop}_t} \tag{7}$$

where, BUA_t and Pop_t represent the built-up area and population at time t, respectively.

Land consumption rate relative to population growth rate (LCRPGR) is defined as the ratio of the rate of land consumption to the rate of population growth (United Nations, 2025). A ratio greater than 1 (LCRPGR >1) indicates that the increase in space consumption exceeds the increase in population. This is a sign of excessive space occupation. In other words, land use is inefficient and unsustainable. This is obtained using Eq. (8).

$$\text{LCRPGR}=\frac{\text{LCR}}{\text{PGR}}=\frac{\text{Ln}\,(\text{BUA}_{t+n}-\text{BUA}_t)}{\text{Ln}\,(\text{Pop}_{t+n}-\text{Pop}_t)} \tag{8}$$

where, BUA_{t+n} and BUA_t represent the built-up area at the end of the study ($t+n$) and the built-up area at the initial time of the study (t), respectively. Pop_t represents the initial population and Pop_{t+n} is the population in the last year of the study.

When the value obtained from this calculation was greater than one, land use was considered inefficient and unsustainable over the study period.

Urban expansion speed evaluates the annual expansion of built-up areas over the different periods considered in this study. This is obtained using Eq. (9):

$$\text{US}=\frac{(\text{BUA}_{t2}-\text{BUA}_{t1})}{(t2-t1)} \tag{9}$$

where, BUA_{t1} and BUA_{t2} represent the built-up areas on dates $t1$ and $t2$, respectively.

Intensity of urban sprawl refers to the extent of built-up area expansion at different times during the study period

(Li et al., 2021). This was calculated using Eq. (10):

$$I=\frac{\mathrm{BUA}_{t2}-\mathrm{BUA}_{t1}}{\mathrm{BUA}_{t1}\times T}\times 100\% \tag{10}$$

where, BUA_{t1} and BUA_{t2} are the built-up areas at dates $t1$ and $t2$, respectively. T represents the time interval considered (i.e., $t2$-$t1$).

2.3.4 Evolution of the CBI

Cities can use the Singapore Urban Biodiversity Index as an assessment tool to compare and track the progress of their biodiversity conservation efforts with their baselines (Secretariat of the Convention on Biological Diversity, 2021). The 2021 version of the Urban Biodiversity Index proposes 28 different indicators for evaluation. This study used indicator 1, which concerns a city's natural space proportion. The urban biodiversity index for Abomey-Calavi was evaluated over four different years (1992, 2002, 2012, and 2022).

The CBI is obtained using Eq. (11) (Secretariat of the Convention on Biological Diversity, 2021):

$$\mathrm{CBI}=\frac{\text{Total natural area}}{\text{Area of city}}\times 100\% \tag{11}$$

Natural areas include restored areas, naturalized areas, forests, mangroves, natural watercourses, and lakes (Secretariat of the Convention on Biological Diversity, 2021).

2.3.5 Temperature trend

Various variables are used to verify the microclimate, such as precipitation, temperature, wind, and humidity (Waseem et al., 2021). This study focuses on temperature data. The temperature data used were obtained from the Institut Géographique Nationale of the Benin Republic (IGN-Bénin). The data used were collected from 1971 to 2022. The half-century study period (half-century) was chosen to ensure a broader view of temperature trends. The data used were obtained from the Cotonou synoptic station (Cotonou lies to the east of the study area). There are two reasons for choosing this station. First, the municipality of Abomey-Calavi does not have its own synoptic station. Second, the municipality of Cotonou, located east of Abomey-Calavi, shares similar climatic conditions.

To assess breaks and determine whether trends were significant over this period, we used the Pettitt test. The Pettitt test is a non-parametric statistical test for identifying abrupt variations in a time series (Das & Banerjee, 2021) and is widely used in environmental sciences and hydrology, among others.

For a time series with a sample size of N, the formula for constructing the statistic is shown in Eq. (12):

$$U_{t,N}=U_{t-1,N}+\sum_{j-1}^{n}\mathrm{sgn}(x_t-x_j) \tag{12}$$

where, t = 2, ..., N. Assuming $x_t-x_j=\beta$, the value sgnβ is determined by Eq. (13):

$$\mathrm{sgn}\beta\begin{cases}+1 & \beta>0\\ 0 & \beta=0\\ -1 & \beta<0\end{cases} \tag{13}$$

3. Results

3.1 Overall Accuracy and Kappa Coefficient

We assessed the overall accuracy of each map to ensure the quality of the results. Classification using the MLC algorithm produced overall variant accuracies between 93.75% and 88.12%, and variant Kappa coefficients between 0.842 and 0.917, as shown in Table 4.

Table 4. Overall accuracy and Kappa coefficient

Years	1992	2002	2012	2022
Coefficient Kappa	0.883	0.842	0.917	0.90
Overall Accuracy	91.25%	88.125%	93.75%	92.5%

3.2 Land Use Land Cover (LULC) and Indicator 11.3.1

3.2.1 LULC

The analysis of the district surface area considers four types of space: water, bare land, vegetation, and built-up areas. The 1992 map showed a predominance of vegetation formations, which accounted for more than 60 percent (62.78%) of the total surface area. They were distributed throughout the district, with concentrations in the southwest region. Surface waters dominate the east and south of the district, accounting for 17.29% of the total land area. Bare land (14.68%) and built-up areas (5.25%) were the least represented in the territory in 1992. They were concentrated in the north and south of the district.

In 2002 (Figure 2b), there was a change in land use compared to 1992. These changes can be observed in three main areas: built-up areas, bare land, and vegetation. The built-up area increased from 5.25% to 16.89% of the total land area in 10 years. The undeveloped land decreased from 14.68% to 6.99% of the total surface area. Vegetation also declined significantly from 62.78% in 1992 to 56.59% in 2002.

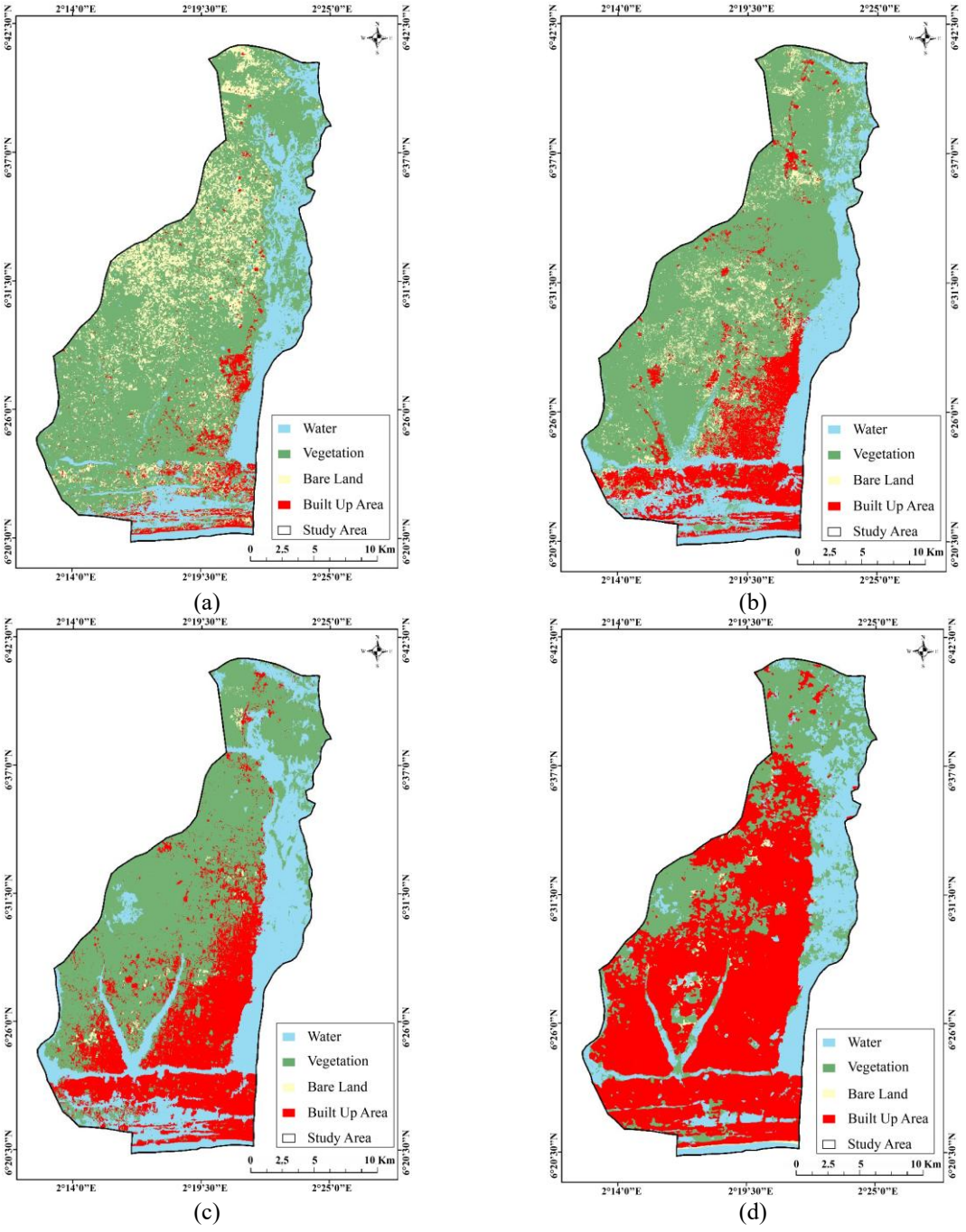

Figure 2. (a) LULC in 1992, (b) LULC in 2002, (c) LULC in 2012, and (d) LULC in 2022

Between 1992 and 2002, the built-up areas increased at the expense of vegetation and bare land. This can also be observed between 2012 and 2022, as illustrated in Figure 2. An analysis of Figures 2c and 2d shows a clear shift in built-up area between 2002 and 2022. From 25.78% to 55.81% during this period, the built-up area occupied an additional 30.03% of the communal surface area. Over the same period, vegetation largely regressed, dropping from 47.97% to 24.00%. Some wetlands are also occupied. The water surface area is expected to decrease from 25.74% in 2012 to 19.16% in 2022. The data from these maps are summarized in Table 5.

Table 5. Change in land use between 1992 and 2022

Spaces	1992		2002		2012		2022	
	Sq km	%	Sq km	%	Sq km	%	Sq km	%
Built up area	26.16	5.25	84.20	16.89	128.53	25.78	278.27	55.81
Water	86.20	17.29	97.38	19.53	128.32	25.74	95.55	19.17
Vegetation	313.03	62.78	282.16	56.59	239.15	47.97	119.68	24.00
Bare Land	73.19	14.68	34.83	6.99	2.57	0.52	5.08	1.02

Overall, from 1992 to 2022 (Figure 3), the surface area of each land use zone changed. There has been significant growth in the built-up area, which has increased from 5.25% to 55.81%, to the detriment of the vegetated area, which has decreased from 62.78% to 24.00%.

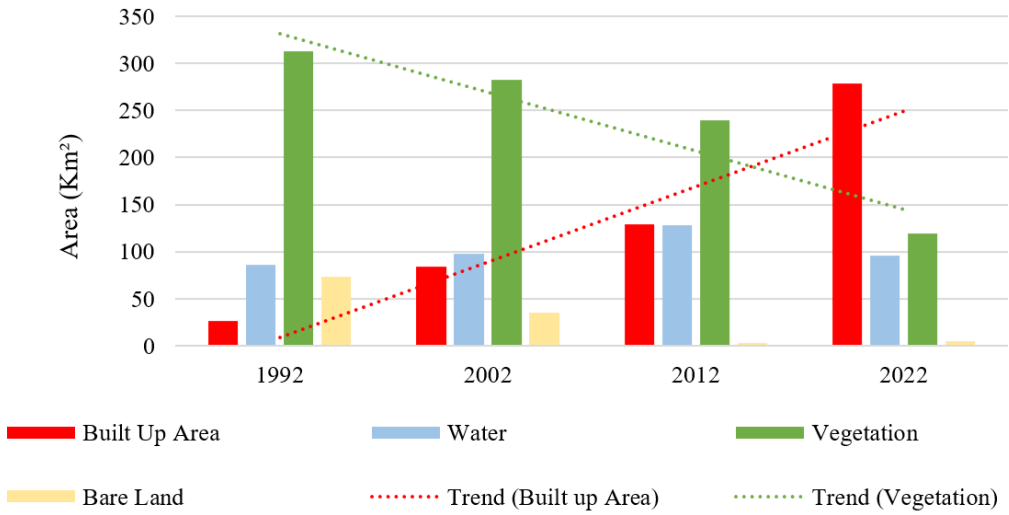

Figure 3. Change in land use between 1992 and 2022

3.2.2 Indicator for SDG 11.3.1 and secondary indicators

Indicators of SDG 11.3.1. Table 6 presents the results of the averaging analysis. The average space consumption during the study period was 0.321. It should be noted that this rate varies from one decade to another. The years 1992-2002 record the highest rate of space consumption (0.222), while the decade 2002-2012 records the lowest (0.053). The space consumption per capita (LCPC) over the study period (1992-2022) was 231.97 m². The decade in which this figure was highest was 2002-2012. This same decade recorded a negative rate of change (-28.4%). This means that, over this decade, the area occupied per inhabitant decreased between the two reference years. Over the entire study period, the ratio of change in occupied space per inhabitant was 12.2%, which means that space consumption per inhabitant increased between 1992 and 2022.

Similarly, the rate of evolution of the built-up area was significant at 8.403 km²/year. This compares with 5.80 km²/year, 4.43 km²/year, and 14.97 km²/year respectively in 1992-2002, 2002-2012, and 2012-2022.

Table 6. ODDs 11.3.1 indicators between 1992 and 2022 in Abomey-Calavi, Republic of Benin

Period	LCR	PGR	LCR/ PGR	LCPC (m²)	Speed (km²/year)	Intensity
1992-2002	0.222	0.089	2.50	206.80	5.804	22.185
2002-2012	0.053	0.076	0.70	273.61	4.433	5.265
2012-2022	0.116	0.060	1.93	195.83	14.973	11.650
1992-2022	0.321	0.075	4.28	231.97	8.403	32.122

Notes: 1. LCR: Land Cover Rate, 2. PGR: Population Growth Rate, 3. LCRPGR: Ratio of Land Cover Rate to Population Growth Rate; 4. LCPC: Land Consumption Per Capita.

Figure 4 shows the evolution of the Land Cover Rate to Population Growth Rate (LCRPGR) between 1992 and 2022.

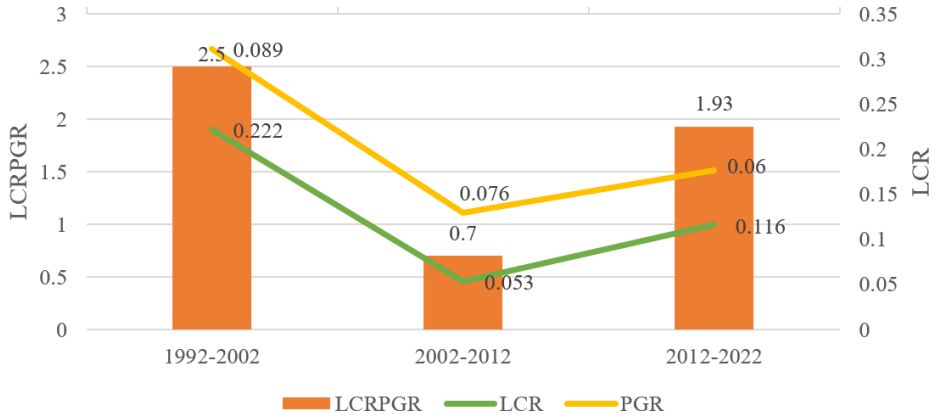

Figure 4. LCRPGR evolution in Abomey-Calavi (1992-2022)

3.3 Evolution of CBI

The evaluation of the urban biodiversity index in the case of Abomey-Calavi considered natural green spaces, natural blue spaces, and bare land. Figure 5 shows the CBI data between 1992 and 2022 and a decline in the biodiversity index from the first to the last year of the study. From 94.75% in 1992, the index fell to 44.19% of the district's area by 2022. Natural areas lost a significant surface area, equivalent to 50.56% of the territory of the district studied. This highlights the need to preserve natural areas throughout cities.

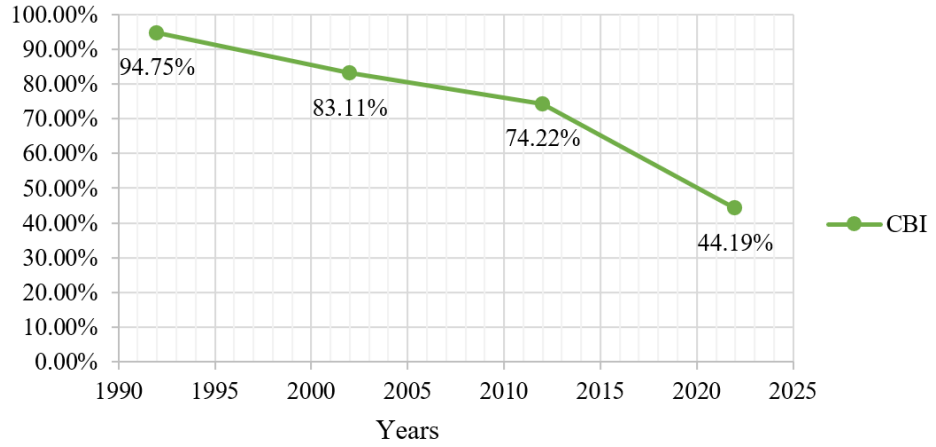

Figure 5. CBI applied to Abomey-Calavi between 1992 and 2022

3.4 Temperature Trend

Figure 6 shows the mean annual temperature trends in Abomey-Calavi from 1971 to 2022. Data were collected from the IGN-Bénin based on the Cotonou Synoptic Station.

The average temperatures recorded over the three decades studied are respectively 27.57°C for 1992-2002, 27.94°C for the decade 2002-2012, and 28.19°C for the decade 2012-2022. Between 1972 and 1982, the average temperature recorded was 26.91°C, compared with 27.81°C between 1982 and 1992. Thus, from the decade 1972-1982 to the decade 2012-2022, the average temperature rose by 1.28°C.

Pettitt's homogeneity test was used to identify breaks in the data series. A break was observed in the maximum temperatures (Tmax) in 1997, with a significance expressed by a p-value of 7.617e-05. The average Tmax rose from 30.30°C before the break to 31.02°C after it. As for the minimum temperatures (Tmin), a break was observed in 2002, with a significant p-value of 3.143e-05. The average Tmin rose from 24.41°C before the break to 25.14°C after. Table 7 summarizes the average temperatures before and after breakage, and shows the significance of the results (p-values).

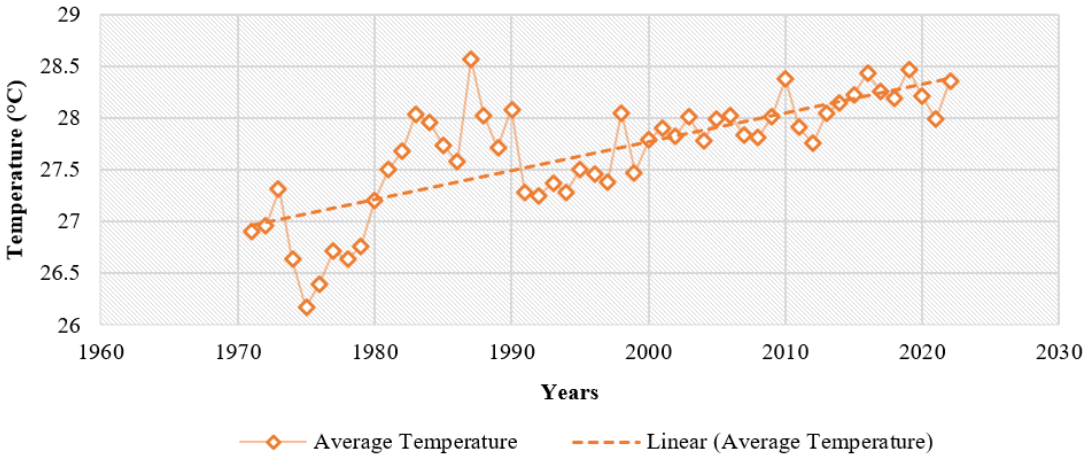

Figure 6. Temperature trend in Abomey-Calavi from 1971 to 2022

Table 7. Pettitt homogeneity test on mean temperatures at Abomey-Calavi between 1971 and 2022

Climatic Parameters	Average Before Rupture (°C)	Average After Rupture (°C)	P-Value
Tmin	24.41	25.14	3.143e-05
Tmax	30.30	31.02	7.617e-05

4. Discussion

The Kappa indices obtained from the analysis of the satellite images were all greater than 0.80, indicating that the maps had excellent accuracy. These results are in line with those of Teadoum Naringué et al. (2025) in the city of Sarh in Chad, where all the calculated Kappa indices were above 0.80. Nevertheless, the results of the present study showed higher Kappa coefficients than those found in the studies of Chaaban et al. (2022) on Syria. The same applies to the results obtained by Wei et al. (2024), where the Kappa indices obtained were sometimes below 0.80.

Studies on the evolution of land use in the city of Abomey-Calavi show rapid growth in built-up areas, with an average rate of 8.403 km²/year over the entire study period, peaking at 14.973 km²/year in the last decade of the study (2012–2022). This suggests that cities are expanding rapidly near the capital cities and other major West African cities. The studies of Asenso Barnieh et al. (2020) showed that the surface area of human settlements doubled between 1975 and 2013 in West Africa and also made this point. In East Africa, and more specifically in Kenya, Greiner et al. (2021) showed a rapid shift in land use towards human activities. This is also the reality of many cities around the world, as Waseem et al. (2021) point out for cities in South Asia and Asia in general.

Analyzing LCPC in a city allows us to determine whether land is used efficiently to promote sustainable urban development. This study found that LCPC in Abomey-Calavi varied from one period to the next. Its average value is 231.97 m²/capita between 1992 and 2022. In the district of Abomey-Calavi, a person needs 231.97 m² of land to live. This value is well above that of other cities on the African continent, such as Nairobi, where one inhabitant requires 21 m² of space to live (Hu et al., 2021). Hu et al. (2021) studied 40 reference cities and showed that the value of space consumed per inhabitant varies from one city to another and in different parts of the same city. They discovered that this difference also applies to different regions of the world; in cities in the Global South, the LCPC is 2.5 times greater than in cities in the Global North.

The evaluation of indicator 11.3.1 of SDGs over different periods makes it possible to assess the progression of land use with the population growth rate. Over the three sub-periods of analysis considered in this study, we can see that the ratio of per capita land consumption to population growth rate gives a value greater than 1 (LCRPCR > 1) for the two periods. These figures (LCRPCR > 1) indicate that land use is inefficient, as the rate of space consumption exceeds that of population growth. Over the entire study period (1992-2022), the LCRPCR was well above 1, which means that the city's expansion presents a real problem of efficiency and sustainability. This phenomenon can be explained by various factors, such as natural population growth and rural exodus, affecting countries in the region. This conclusion is also shared by Combary et al. (2024), who focused on sustainable urban development and the urban biodiversity index in Ouagadougou, Burkina Faso, West Africa. It should be noted that the work of Fonseca (2024) on the localization of the SDGs recommends adapting indicators to local contexts for more sustainable cities. At the same time, Hounsounou (2019)'s work on Abomey-Calavi highlights the rapid evolution of the urban fabric and links this phenomenon to population growth, rural exodus, land availability, and lower cost of living. Cardenas-Ritzert et al. (2024) works on multi-level evaluation of urban expansion across

Africa showed that more than 99% of the agglomerations in Ethiopia present an Indicator 11.3.1 value greater than one, and it is the case also for around 85% of agglomerations in Nigeria. This means that across Africa, the land use is not efficient. In western Germany, the study on SDG Indicator 11.3.1, based on an automated retrospective classification approach, demonstrated that land use change and population growth do not occur concurrently. This is as noticeable in urban areas as it is in some rural ones. This shows that the need for more efficient land use policies globally is crucial. It also highlights the various environmental consequences of rapid urban expansion.

The CBI analysis in this study showed a drastic decrease in biodiversity over the period 1992–2022. This highlights the growing need to preserve urban ecosystems and their biodiversity. This conclusion was also drawn from the work of Combary et al. (2024) on the city of Ouagadougou in Burkina Faso, West Africa. In the same vein, the work of Teadoum Naringué et al. (2025) on the town of Sarh in Chad, Central Africa, showed rapid growth in the built-up area and a rapid decline in vegetation. Moreover, preserving biodiversity has a positive influence that urban ecosystems have on various aspects of urban life (Uchiyama & Kohsaka, 2019). Similarly, the work of Bele & Chakradeo (2021) on perception of biodiversity showed the importance of biodiversity and, more specifically, ecological aesthetics in the process of creating a sustainable urban space. Thus, CBIs can be used to implement appropriate management strategies to preserve urban ecosystems and biodiversity, which in turn can lead to the overall sustainable management of these cities (Uchiyama & Kohsaka, 2019).

The annual temperature varies between 1971 and 2022. Pettitt's homogeneity test showed breaks in the minimum and maximum values recorded. For maximum values, a break was recorded in 1997, with a rise from 30.30°C before the break to 31.02°C after the break. This represents an increase of 0.72°C. For the minimum temperatures, the increase was 0.73°C. In areas characterized by rapid growth in the built-up area, we are seeing an increase in temperature. This is the observation made by Chen et al. (2023). These constantly rising minimum and maximum temperatures can have various consequences for the urban environment and its residents. Putra et al. (2021) revealed a close relationship between urban heat island, land use, and environmental quality in the city of Jakarta. For example, mortality and morbidity are increased by high temperatures (Ebi et al., 2021), vegetation dynamics are influenced by high temperatures. In addition, Lopez et al. (2017) studied atmospheric temperature and pollen content in Abomey-Calavi and revealed a positive correlation between maximum air temperature and biodiversity.

5. Conclusions

Urban sprawl is influenced by various factors and has varying consequences. Environmental consequences are greater when this process is uncontrolled or inefficient. Indicators are therefore being developed to assess not only the efficiency of the urban sprawl process, but also its impact on biodiversity and temperature. In this study, the analysis of land use (LULC) showed the rapid expansion of urban spaces in territories adjacent to capital cities in West Africa. SDG indicator 11.3.1 shows that urban sprawl is inefficient in Abomey-Calavi, as in many other cities in the Global South. This unsustainable spatial evolution implies rapid loss of biodiversity.

Indicator 1 of the Singapore Urban Biodiversity Index applied to the district of Abomey-Calavi shows that, between 1992 and 2022, the natural area disappeared very rapidly. Actions are needed to preserve natural areas and urban biodiversity as a whole.

The breakpoint test performed on the temperature data showed that there was a breakpoint for both the minimum and maximum temperatures. The observed breaks were significant, and representative p-values were recorded. It can be seen that temperatures in the study area, as in many other towns in the Global South, are changing, with a gradual increase in air temperature over the last 50 years.

The results of this study underline that inefficient urban sprawl leads to a rapid loss of urban biodiversity, as well as temperature change. It is important and urgent for researchers, elected representatives, and urban planners to take a perpetual look at the assessment of urban sprawl over the years and its relationship with biodiversity and temperature, understand the consequences of the phenomenon, and propose solutions to overcome the crisis. More specifically, to address the rapid land development and loss of biodiversity in Abomey-Calavi, local authorities should consider implementing clearer zoning regulations that prioritize green spaces and prevent uncontrolled growth. Community-driven projects focused on sustainable farming could transform vacant lots into urban farms. This would help protect native plants and pollinators while boosting local food production. Additionally, launching widespread tree-planting campaigns could improve urban biodiversity, reduce the effects of climate change, and ensure that everyone has access to green spaces. The expected outcome of such an approach is the development of more sustainable cities, less aggressive with the environment, and greater protection of biodiversity and temperature.

Author Contributions

Conceptualization, C.J.M.K.; methodology, C.J.M.K., F.T.N. and M.A.; software, C.J.M.K.; validation, I.D., B.S.A. and A.K.; formal analysis, C.J.M.K.; investigation, C.J.M.K. and M.A; resources, C.J.M.K..; data curation

C.J.M.K. and M.A; writing—original draft preparation, C.J.M.K.; writing—review and editing, C.J.M.K., B.S.A. and A.K.; visualization, I.D., A.K.; supervision, I.D., B.S.A.; project administration, A.K.; funding acquisition, C.J.M.K. All authors have read and agreed to the published version of the manuscript.

Funding

This work is funded by the Regional Centre of Excellence on Sustainable Cities in Africa (CERVIDA-DOUNEDON), the Association of African Universities (AAU), and the World Bank (IDA: 6512-TG & 5360-TG).

Data Availability

The data used to support the research findings are available from the corresponding author upon request.

Conflicts of Interest

The authors declare no conflict of interest.

References

Asenso Barnieh, B., Jia, L., Menenti, M., Zhou, J., & Zeng, Y. (2020). Mapping land use land cover transitions at different spatiotemporal scales in West Africa. *Sustainability*, *12*(20), 8565. https://doi.org/10.3390/su12208565.

Bele, A. & Chakradeo, U. (2021). Public perception of biodiversity: A literature review of its role in urban green spaces. *J. Landscape Ecol.*, *14*(2), 1–28. https://doi.org/10.2478/jlecol-2021-0008.

Cao, Y., Zhang, M., Zhang, Z., Liu, L., Gao, Y., Zhang, X., Chen, H., Kang, Z., Liu, X., & Zhang, Y. (2024). The impact of land-use change on the ecological environment quality from the perspective of production-living-ecological space: A case study of the northern slope of Tianshan Mountains. *Ecol. Inf.*, *83*, 102795. https://doi.org/10.1016/j.ecoinf.2024.102795

Cardenas-Ritzert, O. S. E., Vogeler, J. C., Shah Heydari, S., Fekety, P. A., Laituri, M., & McHale, M. (2024). Automated geospatial approach for sssessing SDG indicator 11.3.1: A multi-level evaluation of urban land use expansion across Africa. *ISPRS Int. J. Geo-Inf.*, *13*(7), 226. https://doi.org/10.3390/ijgi13070226.

Chaaban, F., El Khattabi, J., & Darwishe, H. (2022). Accuracy assessment of ESA WorldCover 2020 and ESRI 2020 land cover maps for a region in Syria. *J. Geovisual. Spatial Anal.*, *6*(2), 31. https://doi.org/10.1007/s41651-022-00126-w.

Chen, X., Wang, Z., Yang, H., Ford, A. C., & Dawson, R. J. (2023). Impacts of urban densification and vertical growth on urban heat environment: A case study in the 4th Ring Road Area, Zhengzhou, China. *J. Cleaner Prod.*, *410*, 137247. https://doi.org/10.1016/j.jclepro.2023.137247.

Cobbinah, P. B. & Aboagye, H. N. (2017). A Ghanaian twist to urban sprawl. *Land Use Policy*, *61*, 231–241. https://doi.org/10.1016/j.landusepol.2016.10.047.

Combary, Y. E. F., Zemo, M. A. T., Hemchi, H. M., & Atchrimi, B. T. (2024). Monitoring and assessing of sustainable development in the urban area of Ouagadougou based on SDG 11.3.1 indicator and the city biodiversity index. *Edelweiss Appl. Sci. Technol.*, *8*(6), 1930–1943. https://doi.org/10.55214/25768484.v8i6.2363.

Das, S. & Banerjee, S. (2021). Investigation of changes in seasonal streamflow and sediment load in the Subarnarekha-Burhabalang basins using Mann-Kendall and Pettitt tests. *Arabian J. Geosci.*, *14*, 946. https://doi.org/10.1007/s12517-021-07313-x.

Ebi, K. L., Capon, A., Berry, P., Broderick, C., De Dear, R., Havenith, G., Honda, Y., Kovats, R. S., Ma, W., Malik, A., et al. (2021). Hot weather and heat extremes: Health risks. *The Lancet*, *398*(10301), 698–708. https://doi.org/10.1016/S0140-6736(21)01208-3.

Emadodin, I., Taravat, A., & Rajaei, M. (2016). Effects of urban sprawl on local climate: A case study, north central Iran. *Urban Clim.*, *17*, 230-247. https://doi.org/10.1016/j.uclim.2016.08.008.

Fonseca, M. J. L. (2024). *Localizing the sustainable development goals: The case of Porto* [Mastersthesis]. Universidade do Porto, Portugal.

Greiner, C., Vehrs, H.-P., & Bollig, M. (2021). Land-use and land-cover changes in pastoral drylands: Long-term dynamics, economic change, and shifting socioecological frontiers in Baringo, Kenya. *Hum. Ecol.*, *49*, 565–577. https://doi.org/10.1007/s10745-021-00263-8.

Hounsounou, M. J. (2019). *Etalement urbain et planification spatiale de la commune d'Abomey-Calavi: Enjeux et défis d'aménagement* [Phdthesis]. Université d'Abomey-Calavi, Bénin.

Hu, J., Wang, Y., Taubenböck, H., & Zhu, X. X. (2021). Land consumption in cities: A comparative study across the globe. *Cities*, *113*, 103163. https://doi.org/10.1016/j.cities.2021.103163.

INSAE. (2016). *Cahier des Villages et quartiers de ville du Département de l'Atlantique (RGPH-4, 2013)*. https://instad.bj/images/docs/insae-statistiques/enquetes-recensements/RGPH/1.RGPH_4/resultats%20finaux/Cahiers%20villages/Cahier%20des%20villages%20et%20quartiers%20de%20ville%20Atlantique.pdf

Konkobo, J. & Somé, Y. S. C. (2023). Dynamique spatio-temporelle de l'état de vitalité du couvert végétal avec l'indice NDVI dans la commune rurale de Kouka, au Nord-Ouest du Burkina Faso. *Ann. Univ. Bucharest Geogr. Ser.*, *71*(1), 131–148. https://doi.org/10.5719/aub-g/72.1/8.

Li, C., Cai, G., & Sun, Z. (2021). Urban land-use efficiency analysis by integrating LCRPGR and additional indicators. *Sustainability*, *13*(24), 13518. https://doi.org/10.3390/su132413518.

Li, G., Fang, C., Li, Y., Wang, Z., Sun, S., He, S., Qi, W., Bao, C., Ma, H., & Fan, Y., et al. (2022). Global impacts of future urban expansion on terrestrial vertebrate diversity. *Nat. Commun.*, *13*, 1628. https://doi.org/10.1038/s41467-022-29324-2

Lopez, T. F., Monique, T. G., Adéline, Z. R., Akpov, A., & Koffi, A. (2017). Caractérisation du contenu pollinique de l'atmosphère de la commune d'abomey-calavi de 2015 à 2017. *Eur. Sci. J.*, *13*(30), 417. https://doi.org/10.19044/esj.2017.v13n30p417.

Olanrewaju, S. D. & Adegun, O. B. (2021). Urban sprawl and housing: A case for densification in Nigerian cities. In *Housing and SDGs in Urban Africa* (pp. 287–299). Springer Singapore. https://doi.org/10.1007/978-981-33-4424-2_16.

Osseni, A. A., Dossou-Yovo, H. O., Gbesso, F. G. H., & Sinsin, B. (2023). GIS-based multi-criteria analysis for selecting suitable areas for urban green spaces in Abomey-Calavi District, Southern Benin. *Land*, *12*(8), 1553. https://doi.org/10.3390/land12081553.

Putra, C. D., Ramadhani, A., & Fatimah, E. (2021). Increasing urban heat island area in Jakarta and it's relation to land use changes. *IOP Conf. Ser. Earth Environ. Sci.*, *737*, 012002. https://doi.org/10.1088/1755-1315/737/1/012002.

Saikrishna, M. & Sivakumar, V. L. (2022). A relative study of estimation of pre-flood area of flood-prone regions using maximum likelihood classifier (MLC) and minimum distance to means classifier (MDM) in Cuddalore District, Tamil Nadu, India. *Int. J. Mech. Eng.*, *7*, 937–949.

Secretariat of the Convention on Biological Diversity. (2021). *Handbook on the Singapore Index on Cities Biodiversity*. https://www.cbd.int/doc/publications/cbd-ts-98-en.pdf

Teadoum Naringué, F., Tob-Ro, N., Sorsy, M. L., Aboudou, J. K. S., Blondel Mgang-yo, A., Sing-Non, B. P., Tombar, A. P., & Hetcheli, F. (2025). Dynamics of built-up areas and loss of vegetation in secondary towns: Case study of Sarh Town in Chad, Central Africa. *Sustainability*, *17*(3), 885. https://doi.org/10.3390/su17030885.

Terfa, B. K., Chen, N., Liu, D., Zhang, X., & Niyogi, D. (2019). Urban expansion in Ethiopia from 1987 to 2017: Characteristics, spatial patterns, and driving forces. *Sustainability*, *11*(10), 2973. https://doi.org/10.3390/su11102973.

Thomas, M. F. & Whittington, G. W. (2023). *Environment and Land Use in Africa*. Taylor & Francis.

Uchiyama, Y. & Kohsaka, R. (2019). Application of the city biodiversity index to populated cities in Japan: Influence of the social and ecological characteristics on indicator-based management. *Ecol. Indic.*, *106*, 105420. https://doi.org/10.1016/j.ecolind.2019.05.051.

UN-Habitat. (2021). *Global indicator framework for the sustainable development goals and targets of the 2030 agenda for sustainable development.* https://unstats.un.org/sdgs/indicators/Global%20Indicator%20Framework%20after%202020%20review_Eng.pdf

United Nations. (2025). *SDG Indicators*. https://unstats.un.org/sdgs/metadata

United Nations Department of Economic & Social Affairs. (2019). *World Urbanization Prospects: The 2018 Revision*. United Nations. https://doi.org/10.18356/b9e995fe-en.

Waseem, L. A., Khokhar, M. A. H., Naqvi, S. A. A., Hussain, D., Javed, Z. H., & Awan, H. B. H. (2021). Influence of urban sprawl on microclimate of Abbottabad, Pakistan. *Land*, *10*(2), 95. https://doi.org/10.3390/land10020095.

Wei, Y., Lu, M., Yu, Q., Li, W., Wang, C., Tang, H., & Wu, W. (2024). The normalized difference yellow vegetation index (NDYVI): A new index for crop identification by using GaoFen-6 WFV data. *Comput. Electron. Agric.*, *226*, 109417. https://doi.org/10.1016/j.compag.2024.109417.

Yiran, G. A. B., Ablo, A. D., Asem, F. E., & Owusu, G. (2020). Urban sprawl in sub-Saharan Africa: A review of the literature in selected countries. *Ghana J. Geogr.*, *12*(1). https://doi.org/10.4314/gjg.v12i1.1.